THE FASEB JOURNAL • RESEARCH • www.fasebj.org

The fibrinolytic factor tPA drives LRP1-mediated melanoma growth and metastasis

Yousef Salama,[*,†] Shiou-Yuh Lin,[*] Douaa Dhahri,[*] Koichi Hattori,[‡] and Beate Heissig[*,§,1]

[*]Division of Stem Cell Dynamics, Center for Stem Cell Biology and Regenerative Medicine, The Institute of Medical Science, The University of Tokyo, Tokyo, Japan; [†]Faculty of Medicine and Health Sciences, An-Najah National University, Nablus, Palestine; and [‡]Center for Genome and Regenerative Medicine and [§]Atopy (Allergy) Center, Juntendo University School of Medicine, Tokyo, Japan

ABSTRACT: The multifunctional endocytic receptor low-density lipoprotein receptor-related protein (LRP)1 has recently been identified as a hub within a biomarker network for multicancer clinical outcome prediction. The mechanism how LRP1 modulates cancer progression is poorly understood. In this study we found that LRP1 and one of its ligands, tissue plasminogen activator (tPA), are expressed in melanoma cells and control melanoma growth and lung metastasis *in vivo*. Mechanistic studies were performed on 2 melanoma cancer cell lines, B16F10 and the B16F1 cells, both of which form primary melanoma tumors, but only B16F10 cells metastasize to the lungs. Tumor-, but not niche cell–derived tPA, enhanced melanoma cell proliferation in $tPA^{-/-}$ mice. Gain-of-function experiments revealed that melanoma LRP1 is critical for tumor growth, recruitment of mesenchymal stem cells into the tumor bed, and metastasis. Melanoma LRP1 was found to enhance ERK activation, resulting in increased matrix metalloproteinase (MMP)-9 RNA, protein, and secreted activity, a well-known modulator of melanoma metastasis. Restoration of LRP1 and tPA in the less aggressive, poorly metastatic B16F1 tumor cells enhanced tumor cell proliferation and led to massive lung metastasis in murine tumor models. Antimelanoma drug treatment induced tPA and LRP1 expression. tPA or LRP1 knockdown enhanced chemosensitivity in melanoma cells. Our results identify the tPA-LRP1 pathway as a key switch that drives melanoma progression, in part by modulating the cellular composition and proteolytic makeup of the tumor niche. Targeting this pathway may be a novel treatment strategy in combination treatments for melanoma.—Salama, Y., Lin, S.-Y., Dhahri, D., Hattori, K., Heissig, B. The fibrinolytic factor tPA drives LRP1-mediated melanoma growth and metastasis. FASEB J. 33, 000–000 (2019). www.fasebj.org

KEY WORDS: cancer · protease · bortezomib · matrix metalloproteinase · plasmin

The global incidence of melanoma continues to increase. Although patients treated with the anti-cytotoxic T lymphocyte antigen-4–targeted agent ipilimumab, the RAS-MAPK inhibitor sorafenib, anti-angiogenesis treatment, immunotherapy, and the proteasome inhibitor bortezomib (BTZ) have demonstrated improvements in response rate and survival, the median duration of these responses are often <1 yr (1, 2). Therefore, novel treatment strategies are needed.

ABBREVIATIONS: BTZ, bortezomib; FACS, fluorescence-activated cell sorting; HRP, horseradish peroxidase; KD, knockdown; LRP, low-density lipoprotein receptor-related protein; MEF, mouse embryonic fibroblast; MMP, matrix metalloproteinase; MSC, mesenchymal stem cell; OE, overexpressing; PAP, plasmin-antiplasmin complex; PDGFR, platelet-derived growth factor receptor; Plg, plasminogen; Plm, plasmin; qPCR, quantitative PCR; rtPA, recombinant tissue plasminogen activator; P/S, penicillin/streptomycin; si, small interfering; WT, wild type; YO, *trans*-aminomethylcyclohexanecarbonyl-l-(*O*-picolyl)tyrosine-octylamide

[1] Correspondence: Division of Stem Cell Dynamics, Center for Stem Cell Biology and Regenerative Medicine, The Institute of Medical Science, The University of Tokyo, 4-6-1, Shirokanedai, Minato-ku, Tokyo 108-8639, Japan. E-mail: heissig@ims.u-tokyo.ac.jp

doi: 10.1096/fj.201801339RRR

The plasminogen (Plg) activator system (3, 4) and the matrix metalloproteinase (MMP) family, play important roles in melanoma progression (5). Tissue plasminogen activator (tPA) and urokinase plasminogen activator can convert Plg, the zymogen form, into the active form plasmin (Plm), which is important for blood clot dissolution. tPA rather than urokinase plasminogen activator is expressed in cell lines established from biopsies of patients with metastatic melanoma (6). The finger domain of the mature form of tPA is involved in tPA binding to fibrin and is necessary to promote fibrinolytic activity (7), whereas the mitogenic functions of tPA have been attributed to the epidermal growth factor–like domain (8).

Low-density lipoprotein receptor-related protein (LRP)1 is involved in endocytosis, lipoprotein metabolism, and proteinases degradation (9, 10). The 515-kDa α-chain of LRP1 binds to cancer-associated proteinases, including tPA and MMPs (11–13) or ligands such as lipoprotein lipase (10, 14). tPA can bind to the krinkle-2 domain of LRP1 (15). LRP1 regulates tumor invasion and metastasis by changing MMP2 and -9 expressions *via* an ERK1/2-dependent signaling pathway (16–18). By interacting with other signaling pathways (*e.g.*, β1 integrin), LRP1 alters cell behavior (19).

Several studies have demonstrated a role for LRP1, in the past also simply known as LRP, a member of the low-density lipoprotein receptor gene family in cancer migration and proliferation (for review, see ref. 20). Studies, including those on melanoma (21, 22), have linked low LRP1 expression to a more invasive phenotype. Another study has described opposite results: LRP1 expression was predominantly detected in glioblastoma and, to a lesser extent, in lower grade astrocytomas (23). A recent study demonstrated that yes-associated protein through a transcription- and promoter-dependent mechanism induces LRP1 expression in melanoma cells (24), suggesting a role for LRP1 in melanoma tumorigenesis. The tPA-LRP1 pathway contributes to epithelial-mesenchymal transition and promotes fibroblast survival (17) and glioblastoma cell migration and invasion (16).

Tumor-associated mesenchymal stroma cells, such as the cancer-associated fibroblasts mesenchymal stem cells (MSCs), smooth muscle cells, myofibroblasts, endothelial cells, pericytes, and inflammatory cells, are recruited to the melanoma tumor bed (25). The tumor niche is recognized as a key factor in the multiple stages of cancer progression, mediating local resistance, immune escape, and metastasis (26). We showed that tPA can expand platelet-derived growth factor receptor (PDGFR) α-MSCs in noncancerous tissues (27).

In this study, we evaluated the regulation and function of the tPA-LRP1 interaction for melanoma progression and the cellular and proteolytic composition of the tumor niche. The findings provide mechanistic proof in mice that the tPA-LRP1 pathway is a critical mediator of melanoma cell growth and lung metastasis.

MATERIALS AND METHODS

Cell line and cell culture

The B16F1 and B16F10 melanoma cell lines [CRL-6475; American Type Culture Collection (ATCC), Manassas, VA, USA] were maintained in high-glucose DMEM with L-glutamine, phenol red (Fuji Film Wako, Osaka, Japan), 10% fetal bovine serum (FBS; GE Healthcare, Chicago, IL, USA), and 1% penicillin/streptomycin (P/S) (Nacalai Tesque, Kyoto, Japan). Both the mouse embryonic fibroblast (MEF)-1 (CRL-2214; ATCC) LRP-1$^+$ MEF-1 and LRP-1–deficient PEA 13 cells (CRL-2216; ATCC) were maintained in high-glucose DMEM containing 10% FBS and 1% P/S. Murine MS-5 and human HS-5 stromal cells were cultured in Iscove's modified Dulbecco's medium (Wako) containing 10% FBS and 1% P/S.

Murine erythroleukemia FBL3 and RAW 264.7 (TIB-71; ATCC) cells were cultured in RPMI-1640 medium containing 10% FBS and 1% P/S. Human A-431 squamous carcinoma cells were cultured in Eagle's minimum essential medium + 2 mM glutamine + 1% nonessential amino acids + 10% FBS. Human melanoma cell line SK-MEL-28 cells were maintained in Eagle's MEM and 10% FBS.

Small interfering RNA and short hairpin RNA–based gene knockdown

For tPA knockdown (KD), 2×10^5 B16F10 and B16F1 cells were seeded in a 6-well plate and transfected the next day with tPA shRNA plasmids (sc-36706-SH; Santa Cruz Biotechnology, Dallas, TX, USA). Puromycin selection (1 μg/ml) was performed on newly transfected short hairpin (sh)tPA KD cells (knockdown efficacy, ~50%). Gene knockdown efficiency in B16F10 or B16F1 cells was determined by quantitative PCR (qPCR). For *LRP1* KD, cells were seeded at a 5×10^4 cells/6-well concentration for 16 h before transfection. After 12 h, the transfection medium was replaced with fresh medium. Specific gene-targeting and control nonspecific-targeting small interfering (si)RNAs were obtained from Thermo Fisher Scientific (Waltham, MA, USA). siRNAs targeting LRP1 or a control sequence were transfected into cancer cells at a final concentration of 100 nM using Lipofectamine RNAiMax Transfection Reagent (Thermo Fisher Scientific). The siRNA target sequences were as follows: si-tPA, 5′-CCA UAGUCCUCAUGGGCAA-3′; si-LRP1, 5′-GCUCAUCUC GGGCAUGAUU-3′; siMMP9: 5′-GCGCUCUGCAUUUCUU-CAA-3′; and si-Ctrl, 5′-GCUCCACAGAGUAUACCUU-3′.

Cloning of human tPA and mouse LRP1

We used mouse brain tissue to clone the mouse LRP1 coding sequence, and HUVECs to clone human tPA into the LV-EF-L3T4-IRES2-EGFP vector. The tPA cloning sequence was *Xho*I, 5′-GGGCTCGAGGAAGCAATCATGGATGCAATGAAGAGA-GGGCT-3′ and *Eco*RV, 5′-TTTGATATCTCACGGTCGCATG-TTGTCACGAATCCAGTCT-3′; and the *LRP1* cloning sequence was LRP1-*Xba*I 5′-TCTAGAGCCCACACCATGCTGACCCC-GCCGTTGCTGCTGCT-3′ and LRP1-*Hpa*I 5′-GTTAACCTAT-GCCAAGGGATCTCCTATCTCGTCTTCAGGT-3′.

tPA lentivirus generation for overexpression of tPA

Vesicular stomatitis virus glycoprotein–pseudotyped lentivirus was prepared as described in Kanegae *et al.* (28) *via* a 3-plasmid system (target vector, pMDL, and vesicular stomatitis virus glycoprotein envelope plasmid) by cotransfection of 293T cells with polyethylenimine (Takara, Shiga, Japan). The following plasmid was used as the mock: LV-EF-L3T4-IRES2-EGFP [kindly provided by Dr. Trono's laboratory (Salk Institute, San Diego, CA, USA) and modified by Dr. Tomoyuki Yamaguchi (Institute of Medical Science, University of Tokyo, Japan)]. The viral supernatant was collected 48 h later, cleared, and stored at −80°C. Viral titration was performed using 293T cells.

Drug treatment *in vitro*

The recombinant human tPA (activacin injection, 6,000,000 IU/10 ml; Kyowa Hakko Kirin, Tokyo, Japan) contains the active ingredient alteplase (1 mg equals 580,000 IU). The catalytically inactive recombinant (r)tPA (MTPA-S481A; Molecular Innovations, Novi, MI, USA) is in single chain form and has the serine of active sites mutated to alanine. Active rtPA and catalytically inactive tPA were used at a concentration of 161.8 μM in *in vitro* cultures. The Plm inhibitor *trans*-aminomethylcyclohexanecarbonyl-l-(*O*-picolyl) tyrosine-octylamide (YO)-2 (MW 595.63 g/mol) (29, 30), provided by Dr. Yoshio Okada (Kobe Gakuin University, Kobe, Japan), was dissolved in sterile DMSO and used *in vitro* at a concentration of 10 μM. BTZ (MW 384.24 g/mol; 2204; Cell Signaling Technology, Danvers, MA, USA) was dissolved in DMSO and added to *in vitro* cultures at concentrations ranging from 5 to 20 nM. The MMP inhibitor MMI270 (MW 393.458 g/mol, dissolved in DMSO; Novartis, Basel, Switzerland) was used at a final concentration of 10 nM. The ERK1/2 inhibitor PD98059 (Selleckchem, Houston, TX, USA) was added at a concentration of 50 μM.

Cell culture

B16F10 (5×10^4 cells/well) and B16F1 (1×10^5 cells/well) cells were seeded in 6-well plates (TPP, Trasadingen, Switzerland) for 16 h overnight. Cells were cultured an additional 24 h after adding human rtPA (1500 IU/ml) in PBS (control) in the presence or absence of the MMP inhibitor MMI270.

B16F10 cells (1×10^5 cells/well) were seeded overnight and then cultured in the absence or presence of BTZ (5, 10, and 20 nM) or DMSO controls for 24 h. In another set of experiments, LRP1 silencing was achieved in B16F10 and B16F1 cells by using siRNA (10×10^4 cells/well). Knockdown efficacy 12 h after LRP1 silencing was determined by qPCR or Western blot analysis. In some experiments, siLRP1 KD cells were given fresh medium and then subjected to the mentioned treatment conditions.

B16F10 wild-type (WT; 5×10^4), tPA overexpressing (OE)/KD, or fibroblast cells were seeded in triplicate in 6-well plates and incubated in the presence of specified treatments. Viable cells were counted at 24 and 48 h using trypan blue dead-cell exclusion dye (207-17081; Fuji Film Wako).

Cells were collected with Trizol (Thermo Fisher Scientific) at various time points after treatment for RNA extraction.

mRNA expression using qPCR

Parts of tumor tissues were crushed and filtered for RNA extraction. Total RNA was extracted from cell lines by using Trizol. The purity and concentration of the extracted RNA were analyzed with a spectrophotometer before cDNA generation, according to the manufacturer's protocol. cDNA was generated with the High Capacity cDNA Reverse Transcriptase Kit (Thermo Fisher Scientific) and was stored at −30°C. PCR mixtures (20 μl final volume) contained 10 μl Sybr green mix (TB Green Premix Ex Taq II (Tli RNaseH Plus; Takara), 2 μl 5 ng/μl template cDNA, 0.4 μl 10 μM forward and reverse primer mix (Fasmac, Kanagawa, Japan), and 7.6 μl water. mRNA expression was quantified by performing qPCR using the Step One Plus Real-Time PCR System (Thermo Fisher Scientific), and relative gene expression was given using the $2^{-\Delta\Delta Ct}$ method. β-Actin was used as an endogenous control for normalization if not otherwise stated. The respective forward and reverse primers used for qPCR were murine (m)LRP1: forward 5′-GGACCACCATCGTGGAAA-3′, reverse 5′-TCCCAGCCACGGTGATAG-3′; human (h)LRP1: forward 5′-GATGAGACACACGCCAACTG-3′, reverse 5′-CGGCACTGGAACTCATCA-3′; mtPA: forward 5′-GCCTGGGCAGACACAATTA-3′, reverse 5′-CTTCATCACATGGCACCAA-3′; htPA: forward 5′-AGCTGTGGGGAGCTCAGA-3′, reverse 5′-CACAGCGTCCCTTAAATTCAC-3′; and mMMP9: forward 5′-AGACGACATAGACGGCATCC-3′, reverse 5′-TCGGCTGTGGTTCAGTTGT-3′.

Western blot analysis

Protein crude was recovered by Cell Lysis Buffer (10×; 9803; Cell Signaling Technology). Cell lysates (2–50 μg proteins) were applied on 10% acrylamide gel, transferred to PVDF membrane (MilliporeSigma, Burlington, MA, USA), blocked, and stained overnight at 4°C for LRP1 (sc-16166), tPA (sc-15346), and MMP9 (sc-6840) (Santa Cruz Biotechnology); and β-actin (4967) and p-ERK (4370; Cell Signaling Technology). Membranes were stained with secondary antibody conjugated with horseradish peroxidase (HRP) (rabbit-HRP or goat-HRP; Nichirei Biosciences, Tokyo, Japan) and developed with the ECL Plus detection system (RPN2132; GE Healthcare Life Sciences, Little Chalfont, United Kingdom) using an image analyzer (Image-Quant LAS4000; GE Healthcare Life Sciences).

MSC analysis

Tumor single cells were resuspended in 1 ml ice-cold HBSS/2% FBS and stained for 30 min with the following mAbs: allophycocyanin-conjugated PDGFRα, PE-conjugated Sca-1, PECY7 CD45, and Pacific blue-TER119. All mAbs were purchased from eBioscience (San Diego, CA, USA). Flow cytometry analysis and sorting were performed on flow cytometers (FACS Verse and FACS Aria; BD Biosciences, San Jose, CA, USA). Propidium iodide fluorescence was measured and positive cells (dead cells) were excluded. MSC isolation and culture from bone marrow cells were performed, as described by Dhahri *et al.* (27).

Scratch assay

MSCs (6×10^4) were seeded in a 6-well plate in the growth medium. At subconfluence, a scratch was performed vertically with a sterile yellow pipette tip. Wells were washed gently with PBS. B16-conditioned medium (αMEM basis) was added. Images were taken at 24, 48, and 72 h during wound closure and analyzed with ImageJ software [National Institutes of Health (NIH), Bethesda, MD, USA]. Transfected (mock, tPA OE, and tPA KD) and nontransfected B16F10 cells were cultured in 6-well plates (5×10^4 /well) with complete DMEM. When the cells were confluent, a 1-ml pipette tip spearhead was used to scratch the 6-well plate perpendicular to its bottom, with ∼2 lines of similar width per well. After the plate was washed gently with PBS 3 times, complete DMEM was again applied.

In another set of experiments, siRNA-transfected B16F10 cells were used. B16F10 cells were seeded in 6-well plates (5×10^4 /well) with complete DMEM. The cells were transfected with siRNAs 16 h after the initial seeding. After the transfection medium was replaced the cells reached confluence, scratches were performed as described above.

Images of the scratch wounds were taken using an Olympus Fluorescence BX51 Microscope (Tokyo, Japan) at 0 and 24 h, and the number of cells proliferating or migrating into 6 high-power fields from each scratch were quantified.

Zymography

Plasma samples of tumor-bearing mice retrieved on d 12 were diluted with loading buffer, and samples were loaded on gels containing 7.5% acrylamide (Nacalai Tesque) along with ∼1.345 mg/ml gelatin (Nacalai Tesque). Seven microliters of protein ladder (Bio-Rad, Hercules, CA, USA) was used for each gel. Zymography gels were run at 70 V for 30 min and then at 80 V for 120 min. The gels were incubated for 1 h in Triton X-100–containing washing buffer and for 21 h in a developing buffer at 37°C on a shaker. After the gels were developed, a Coomassie brilliant blue–containing solution was used to stain the gels. The gels are then scanned and further analyzed with ImageJ (NIH).

ELISA

ELISA kits were used to measure murine plasma samples for tPA (Innovative Research, Novi, MI, USA), MMP9 (R&D Systems, Minneapolis, MN, USA), and Plm-anti-Plm (PAP) complex (Cusabio Biotech, Wuhan, China).

Mice

C57/Bl6 mice were purchased from Japan SLC (Hamamatsu, Japan). Six- to eight-week-old age- and sex-matched mice were

used in the experiments. WT $tPA^{+/+}$ and knockout tPA ($tPA^{-/-}$) mice were used after more than 10 backcrosses onto a C57BL/6 background. Animal procedures were performed in accordance with institutional protocols and were approved by the Institutional Animal Care Animal Care and Use Committee of the Institute of Medical Science of the University of Tokyo.

In vivo melanoma model

Mock, tPA OE, tPA KD, and WT B16F10 or B16F1 cells were washed twice with PBS (90% viability, as determined by trypan blue exclusion) and then were inoculated on d 0 (5×10^6/200 μl/mouse, s.c.) into mice, and tumor growth was observed. Mice were euthanized when they showed signs of severe pain, had body weight loss >20% when compared to the initial body weight, or appeared moribund. Tumor growth was monitored daily. Extracted tumors were weighed on d 12.

B16F10 (5×10^4/0.2 ml of PBS) or B16F1 (1×10^5/0.2 ml of PBS) cells were inoculated into the lateral vein of the tail (pulmonary metastasis model). Twelve days after subcutaneous and intravenous tumor cell inoculation, the animals were euthanized by cervical dislocation, and tumors and adjacent conjunctive tissues were removed. Pulmonary nodules were documented with a camera.

Tissue staining

Tissues were fixed in neutral buffered formaldehyde (4%) overnight at 4°C. Sections were subsequently stained with hematoxylin and eosin.

B16F10 cells were cultured on tissue culture slides (Falcon; Thermo Fisher Scientific) until confluence. The slides were fixed with ice-cold methanol and incubated with primary antibody against LRP1 (sc-16166) and tPA (sc-15346) (Santa Cruz Biotechnology). After 2 washes, the cells were incubated for 1 h at room temperature with Alexa Fluor 488 rabbit anti-goat IgG (for LRP1 cells) and Alexa Fluor 488 donkey anti-rabbit IgG (for tPA cells). Sections were counterstained with DAPI, and the slides were analyzed with an upright fluorescence microscope (Olympus).

Statistical analysis

All experiments were performed at least 3 times. Data are means ± SEM. Student's *t* test or ANOVA with Tukey's honest significant difference *post hoc* test were performed with the R program (The R Foundation, Vienna, Austria; *https://www.r-project.org/*). Values of $P < 0.05$ were considered statistically significant.

RESULTS

tPA promotes B16F10 melanoma cell proliferation and migration

We determined tPA expression in various cell lines, including human and mouse melanoma cells, by qPCR (**Fig. 1*A***). HUVECs (positive control for tPA) highly expressed tPA, whereas low tPA expression was found in the murine leukemia cell line FBL3 and the murine macrophage cell line RAW264.7. tPA was highly expressed in the MEF-1 cells. Confirming previous reports (6), tPA expression was found in the human melanoma cell lines A-431 and SK-MEL-28 and in the murine low metastatic melanoma B16F1 cells. The highly metastatic B16F10 melanoma cells (31) showed higher tPA expression than the less aggressive B16F1 cells.

To examine the effects of tPA on melanoma growth, we treated B16F10 cells with recombinant enzymatically active and inactive forms of tPA. Enzymatically active and inactive rtPA (Fig. 1*B*) enhanced proliferation, whereas plasmin inhibitor treatment (YO2 and tranexamic acid) in a dose-dependent manner prevented tPA-induced cell proliferation (Fig. 1*C, D*). We next overexpressed tPA by using lentivirus (tPA OE) or knocked down tPA with shRNA (tPA KD) in B16F10 cells, and confirmed tPA expression by Western blot analysis (Fig. 1*E*). tPA expression in tPA OE and tPA KD cells was confirmed by qPCR. tPA OE enhanced cell proliferation, whereas tPA KD suppressed B16F10 proliferation when compared to the appropriate controls (Fig. 1*F*). These data demonstrated that tPA and Plm enhance melanoma cell proliferation.

To investigate a possible role for tPA in controlling melanoma cell migration, tPA OE cells were subjected to a migration assay. Higher migratory ability was found for tPA OE cells when compared to mock controls (Fig. 1*G*).

tPA-induced ERK1/2 activation involves LRP1

Proteolytically active and inactive tPA can signal through the LRP1 receptor (9). B16F10, MS-5 stromal cells, LRP1 WT MEF-1 cells, but not LRP1-deficient PEA 13 fibroblasts (negative control) expressed LRP1 (**Fig. 2*A***). It has been reported that the protease-independent mitogenic effect of tPA requires LRP1 (32). Therefore, we examined the role of LRP1 in the effects of tPA on cell proliferation and migration. B16F10 LRP1 knockdown by gene silencing resulted in a >90% gene knockdown of LRP1 mRNA expression, as determined by qPCR, and of LRP1 protein expression, as determined by Western blot analysis (Fig. 2*C*). tPA enhanced proliferation of LRP1 WT MEF-1, but not of LRP1-deficient PEA 13 or B16F10 LRP1 KD cells (Fig. 2*B–D*). Similarly, tPA-induced melanoma cell migration was blocked in siLRP1 cells (Fig. 2*E*). These data suggest that LRP1 mediates tPA-induced melanoma cell proliferation and migration.

MMP9-mediated cell proliferation requires LRP1

LRP1 promotes glioblastoma cell migration and invasion by regulating the expression and function of MMP2 and -9 through an ERK-dependent signaling pathway (16). ERK phosphorylation and MMP9 protein expression were increased in tPA OE cells, but not in siLRP1 KD cells, or cells treated with the Plm inhibitor YO2, as shown by Western blot analysis (**Fig. 3*A***). tPA-induced cell proliferation required ERK1/2 activation, as shown using an ERK1/2 inhibitor (ERK1/2 PD98059; Fig. 3*B*). These data unveil an additional regulation of tPA-driven cell proliferation through ERK1/2 activation.

We next investigated the mechanism by which tPA and LRP1 alter melanoma cell proliferation and migration. MMP9 is a key protease involved in melanoma metastasis.

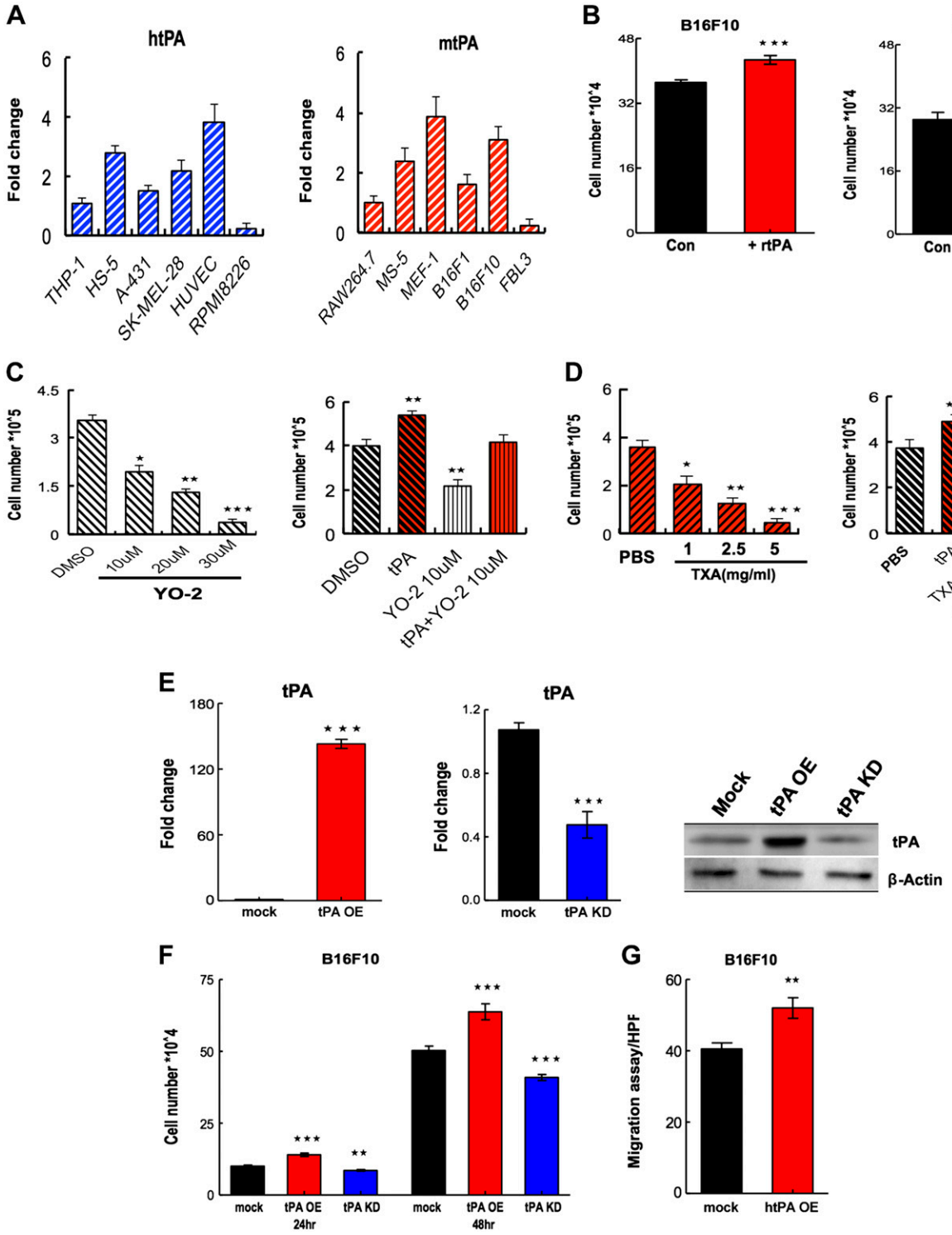

Figure 1. tPA enhances melanoma cell proliferation and migration. *A*) Human (A-431, SK-MEL-28) and murine melanoma cells (B16F1, B16F10) were analyzed by qPCR for *tPA* mRNA expression ($n = 3$/group). Controls included primary HUVECs, stromal and fibroblastic cells, such as human HS-5, murine MS-5, and myeloid (THP-1, RAW264.7). Transcript levels were normalized to β-actin. Graphs represent averages from 3 to 7 independently prepared templates. The data represent 3 independent experiments with similar results. *B*) Cultured B16F10 cells treated with rtPA or not (left) or inactive rtPA (right) were counted after 24 h ($n = 10$). *C, D*) B16F10 cells were treated with various concentrations of the Plm inhibitors YO2 (*C*) or tranexamic acid (*D*), with or without the addition of rtPA. Cells were counted after 24 h ($n = 10$). *E*) *tPA* expression was determined in B16F10 cells stably tPA OE, control (mock), and tPA KD, with qPCR (left, middle), and Western blot analysis (right). *F*) Proliferation of tPA OE, tPA KD, and mock B16F10 cells after 24 and 48 h in culture. *G*) Scratch assay using mock or tPA OE B16F10 cells ($n = 10$). Each data point represents triplicate experiments. Each experiment was repeated at least twice, and the combined data are shown. Means ± SEM. $^*P \leq 0.05$, $^{**}P \leq 0.01$, $^{***}P \leq 0.001$ (Student's *t* test).

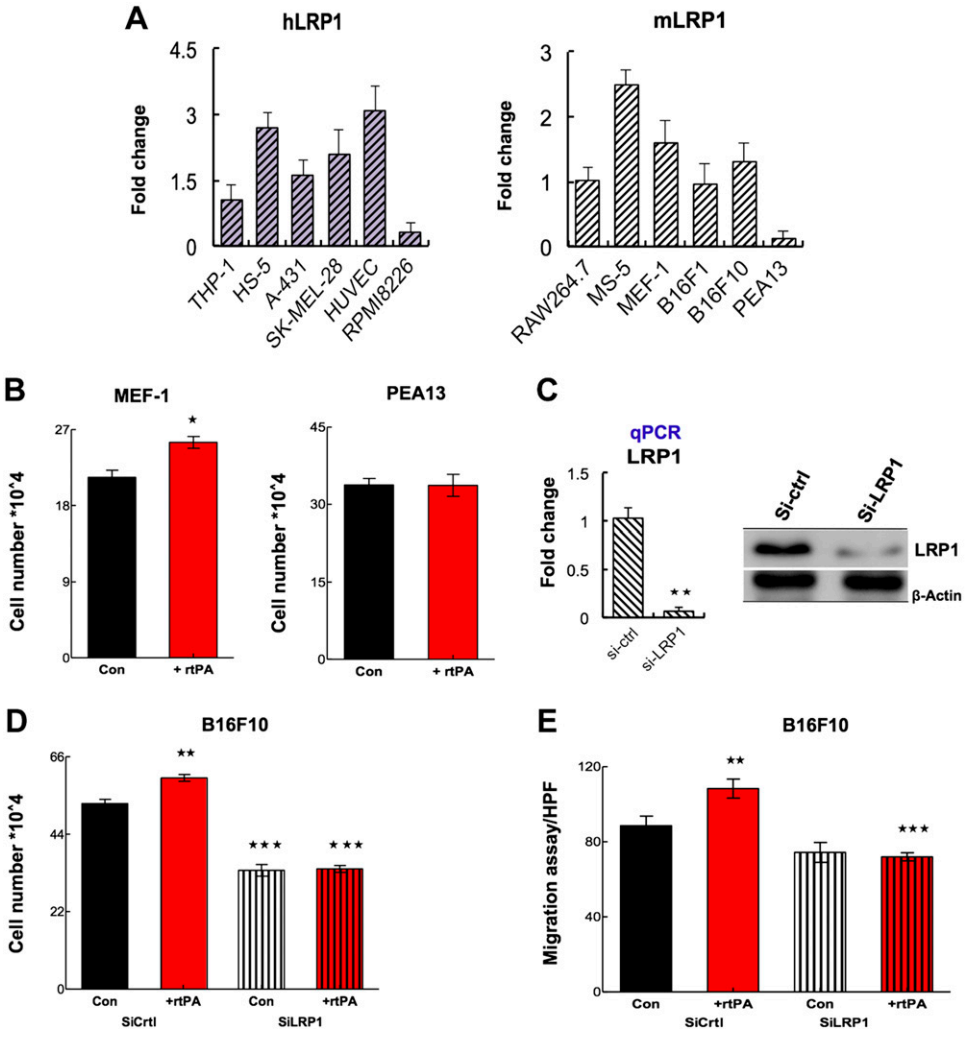

Figure 2. LRP1 controls tPA-mediated melanoma proliferation. *A*) Representative LRP1 expression of human (left) and mouse (right) on THP-1, HS-5, A-431, SK-MEL-28, HUVECs, and RPMI28 cells by using qPCR. β-Actin served as a reference gene. *B*) Cell growth of LRP-1 WT MEF-1 and LRP1-deficient PEA 13 cells and B16F10 control (siCrtl) or B16F10 LRP1 gene-silenced (siLRP1) cells cultured in the absence or presence of rtPA. *C*) LRP1 silencing in B16F10 cells was confirmed by qPCR (left; transcript levels were normalized to β-actin) and Western blot analysis (right; β-actin served as control). *D*) Cell growth of B16F10 control (siCrtl) or B16F10 LRP1 gene-silenced (siLRP1) cells cultured in the absence or presence of rtPA. *E*) LRP1 silenced or control B16F10 cells were subjected to a scratch assay in the presence or absence of rtPA. The average of migrated cells was determined from 6 high-power fields/well in images taken after 24 h. Each experiment was repeated at least twice and the combined or representative data are shown. Each data point represents triplicate experiments. Experiments were repeated at least twice. Data are means ± SEM. $*P \leq 0.05$, $**P \leq 0.01$, $***P \leq 0.001$ (Student's *t* test).

Because LRP1 regulates MMP expression (33, 34), we next asked whether activation of the tPA-LRP1 pathway regulates MMP9 expression in B16F10 cells. rtPA-treated and tPA OE cells, but not tPA KD cells, showed increased MMP9 expression when compared to untreated controls (Fig. 3*C*). Gene silencing of LRP1 reduced MMP9 and tPA expression (Fig. 3*D*), indicating that LRP1 controls endogenous MMP9 and tPA expression.

Next, we explored the importance of MMP9 for LRP1-mediated tPA gene expression. MMP9 knockdown in B16F10 cells was confirmed (Fig. 3*E*). siMMP9 decreased (Fig. 3*F*), whereas the addition of recombinant MMP9 upregulated tPA expression in B16F10 cells, a process that required the presence of LRP-1 (Fig. 3*G*). Our data implicate that LRP1 serves as a gatekeeper for tPA-induced MMP9 and tPA expression.

To elucidate the role of MMP9 and LRP-1 in tPA-mediated cell proliferation, we treated B16F10 cells with different concentrations of recombinant MMP9. MMP9 used at both at low (10 ng) and high (100 ng) concentrations increased B16F10 proliferation (Fig. 3*H*), whereas MMP9-mediated cell proliferation was abolished in LRP1 KD cells (Fig. 3*I*). tPA-driven cell proliferation through LRP1 required the presence of MMP9 as shown using MMP9 KD cells (Fig. 3*J*).

To investigate the role of MMP9 for tPA-induced proliferation and migration, B16F10 cells were treated with the broad range inhibitor MMI270. MMI270 alone blocked tPA-enhanced B16F10 proliferation in a dose-dependent manner (Fig. 3*K*). Similarly, MMI270 impeded tPA-induced B16F10 migration (Fig. 3*L*). Plm inhibition by YO2 alone did not block migration of untreated B16F10 cells, but inhibited tPA-induced melanoma cell migration, indicating that the tPA migration-promoting effects required active Plm (Fig. 3*N*). The findings suggest a mechanism whereby tPA by interacting with melanoma LRP1 enhances MMP9-mediated melanoma cell migration and proliferation.

tPA-LRP1 signaling induces tumorigenesis and lung metastasis *in vivo*

Next, we investigated whether tPA enhances LRP1-mediated tumorigenesis *in vivo*. We transplanted tPA

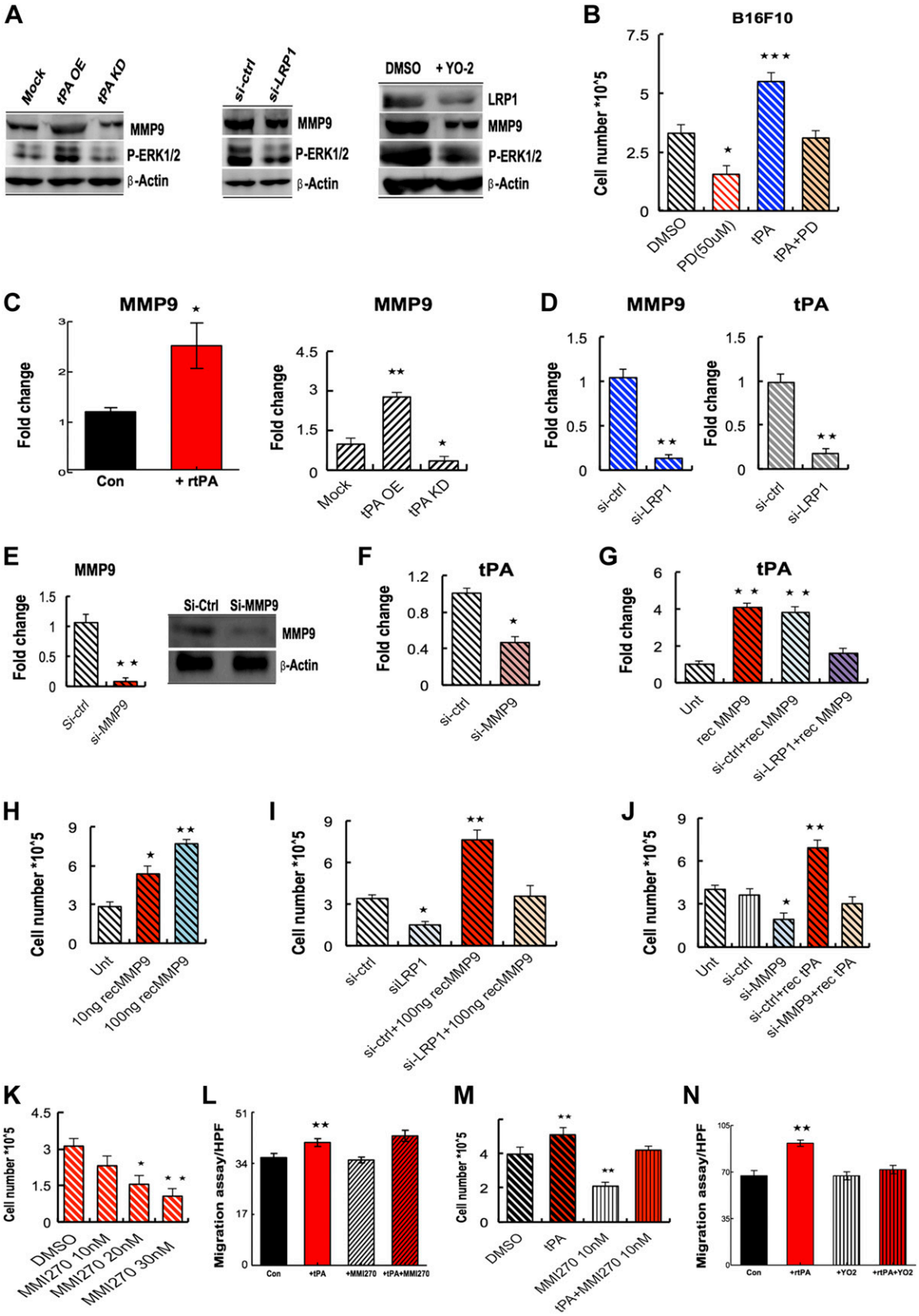

Figure 3. MMP9 is a critical target of tPA-LRP1 signaling in melanoma cells. *A*) Western blot analysis of LRP1, pERK1/2, MMP9, and the loading control β-actin in mock, tPA OE, tPA KD, si-ctrl, siLRP-1, DMSO-treated, and YO2-treated B16F10 cells. *B*) B16F10 cells were treated with rtPA in the presence or absence of the ERK1/2 inhibitor PD98059, and the number of cells was determined. *C*) *MMP9* expression was determined in B16F10 cells cultured for 24 h with rtPA and in B16F10 cells stably tPA OE, control (mock), and after tPA KD by qPCR. *D–J*) LRP1 (siLRP1) and MMP9 gene silencing (siMMP9) was achieved by using

(*continued on next page*)

OE, KD, or mock control B16F10 cells subcutaneously into C57/Bl6 mice. Tumor growth was impaired in tPA KD–injected and Plm inhibitor-treated mice, as well as in mice injected with siLRP1 KD tumor cells, whereas tumor growth was accelerated in tPA OE–injected mice when compared with those in the controls (**Fig. 4*A–C***). LRP1 protein was detected in the collected tumors by Western blot analysis (Fig. 4*C*). Similar to tumor growth variations showing larger error bars, we found variations of LRP1 protein detected in LRP1 WT and KD tumor samples retrieved from different mice. One representative Western blot is shown. Histologic examination 12 d after cell inoculation demonstrated vast areas of necrosis in siLRP1 and tPA KD tumor tissues and in tumor tissues derived from Plm inhibitor-treated mice and bleeding (Fig. 4*D*). Although tPA OE tumor-bearing mice showed an increase in circulating tPA, MMP9 and active Plm (PAP), tPA KD, or siLRP1 tumor-bearing mice showed lower tPA, MMP9, and PAP levels (Fig. 4*E*). An increase in active MMP9 was detected in plasma samples collected 12 d after tumor inoculation of tPA OE, but not mock or tPA KD-injected mice by gelatin zymography (Fig. 4*F*). These data suggest that tPA in part through LRP1 enhances expression and enzymatic activity of MMP9 in melanoma cells, and controls circulating tPA and Plm levels.

It has been reported that tPA-transfected D5.1G4 melanoma cells exhibited extensive pulmonary metastases in a murine intraocular melanoma model (35). Given the robust metastatic phenotypes exerted by LRP1 and tPA in the migration assays *in vitro*, we next investigated the impact of genetic deletion of tPA and LRP1 on lung metastasis in murine melanoma models. To determine whether tumor-derived tPA increases lung metastasis, and, if so, whether LRP1 would mediate this effect, we injected tPA OE, tPA KD, and mock cells intravenously into C57/Bl6 mice. Mice injected with tPA OE, but not tPA KD, cells showed more lung metastatic lesions (Fig. 4*G*). LRP1 gene silencing in tPA OE tumor cells suppressed tPA-driven increased lung metastasis. LRP1 knockdown in WT B16F10 tumor cells reduced lung metastasis in B16F10 cells (Fig. 4*H*). Reduced LRP1 expression in mouse lung lysates of siLRP1-inejcted mice was found, compared with siCtrl-injected mice, as determined by Western blot analysis. Our findings reveal that tPA-LRP1 activation promotes lung metastasis in melanoma cells.

LRP1 and tPA restoration enhance melanoma growth and lung metastasis

B16F1 but not B16F10 cells have poor metastatic potential when injected intravenously into mice. We identified lower *tPA* gene expression in B16F1 than B16F10 cells (see Fig. 1*B*). In the following sets of experiments, the role of tPA and LRP1 on tumor growth and metastasis was examined by using the tPA low-expressing B16F1 cells. B16F10 cells showed a higher proliferation rate when compared to B16F1 cells (**Fig. 5*A***). The addition of rtPA or inactive tPA to tPA low-expressing B16F1 cultures significantly enhanced cell proliferation (Fig. 5*B*), supporting our initial findings in B16F10 cells that tPA can enhance tumor cell growth.

Migration and invasion are controlled by proteases such as tPA and MMP9. Given our initial findings that LRP1 expression controls melanoma growth and migration, we queried whether LRP1 downregulation in B16F1 cells could change the expression of MMP9 and tPA. LRP1 knockdown on B16F1 cells was confirmed (Fig. 5*C*) and reduced the expression of *MMP9*, as determined by qPCR, when compared to controls.

More tPA was found in supernatants from B16F10, but not B16F1, cultures as determined by ELISA (Fig. 5*D*). LRP1 knockdown in B16F10 cells did not change tPA protein secretion into culture supernatants, as determined by ELISA.

Having shown that LRP1 and tPA knockdown reduced the proliferation of B16F10 cells, we examined the cellular behavior and protease gene expression in the tPA low-expressing B16F1 cells after tPA and LRP1 OE. LRP1 and tPA OE in B16F1 and B16F10 cells enhanced cell proliferation *in vitro* (Fig. 5*E*) and enhanced tPA, LRP1, and MMP9 expression, as determined by qPCR (Fig. 5*F*). Increases in protein expression in LRP1 and tPA OE cells was corroborated by Western blot (Fig. 5*G*). Of interest, highest LRP1, tPA, and MMP9 expression was found in tPA- and LRP1-coexpressing B16F1 cells. Given that ERK1/2 is a downstream target of LRP1, we hypothesized that LRP1 and tPA reintroduction leads to enhanced ERK1/2 activation, which indeed was the case. These data suggest that LRP1 and tPA restoration in B16F1 cells may generate tumor cells with higher proteolytic activity and possibly a higher metastatic potential.

To investigate the consequences of LRP1 and tPA OE *in vivo*, we used the subcutaneous tumor model using B16F1 cells (Fig. 5*H–M*). tPA or LRP1 single OE in B16F1 cells led

siRNA. *D*) qPCR measurement of mRNA levels of MMP9 and tPA in siLRP1 or siCtrl control cells. *E*) MMP9 expression was determined in B16F10 KD (siMMP9) and control cells by qPCR (left) and by Western blot analysis. *F*) tPA expression in siMMP9 and control cells by qPCR. *I*) siLRP1 and control cells (siCtrl) were treated with rMMP9 or not treated. *G*) qPCR measurement of mRNA levles of tPA. *H*) B16F10 cells were treated with indicated doses of rMMP9. Cells were counted after 24 hrs. Cell proliferation was assessed after addition of rMMP9 in B16F10 LRP1 KD or control cells. *J*) Cell proliferation was determined in siMMP9 B16F10 or control cells cultured with or without tPA. *K*) Proliferation of B16F10 cells treated with MMI270 or not treated after 24 h in culture. *L,N*) In scratch assays, cells were seeded in 6-well plates, and the cell monolayer was wounded manually. The average of migrated cells was determined from 6 high-power fields/well in images taken after 24 h. *L*) Scratch assay performed using B16F10 cells exposed to rtPA with or without the MMP inhibitor MMI270. *M*) Proliferation of B16F10 cells treated with rtPA, with or without MMI270, after 24 h in culture. *N*) Scratch assay performed in B16F10 cells exposed to rtPA, with or without the Plm inhibitor YO2. Data represent means ± SEM. Experiments were repeated at least twice. $*P \leq 0.05$, $**P \leq 0.01$ (Student's *t* test).

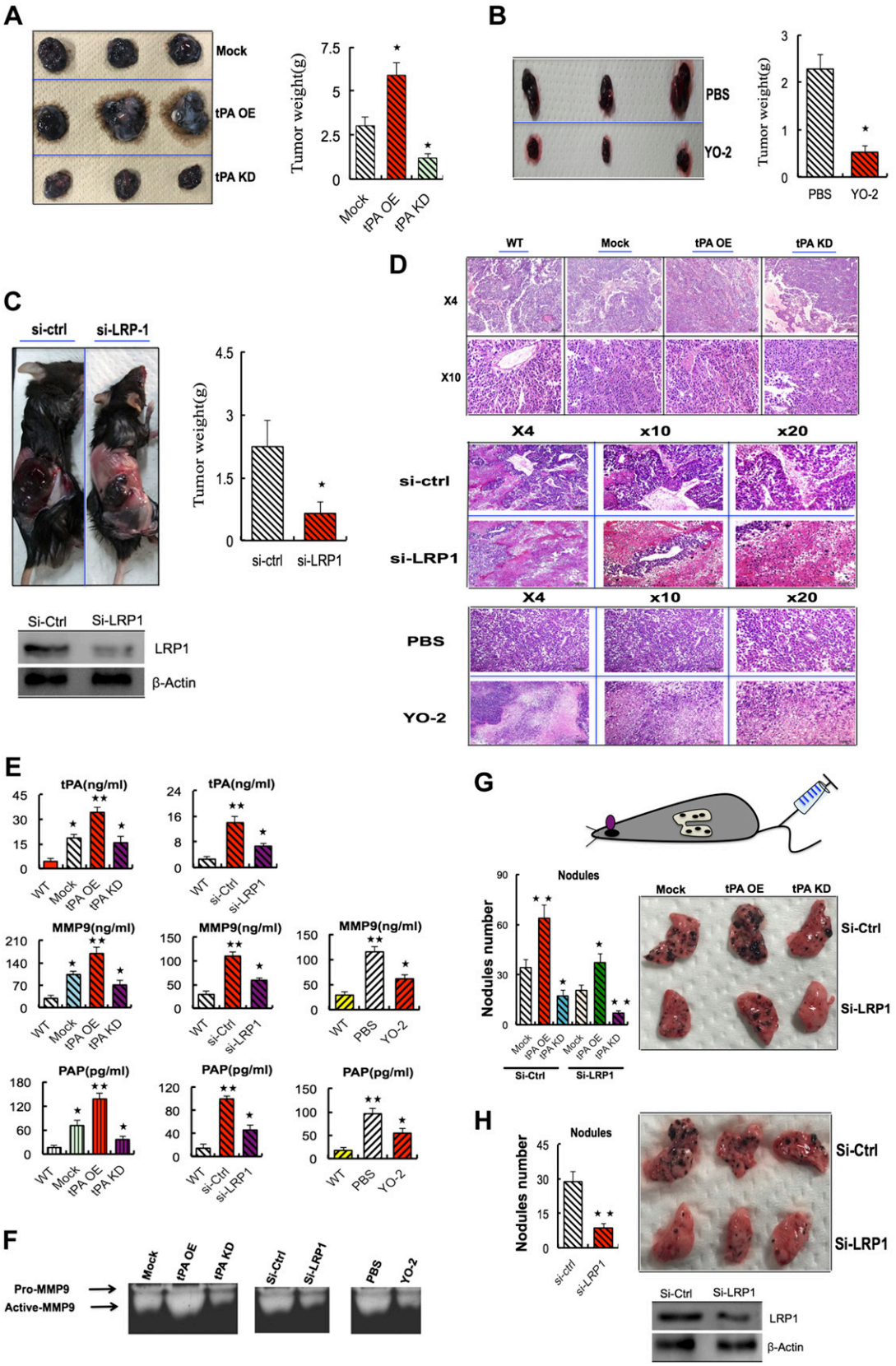

Figure 4. tPA-LRP1 signaling augments melanoma growth and metastasis. *A*) Mock, tPA OE, or tPA KD B16F10 cells (10^6) were injected subcutaneously into the right flanks of C57Bl6 mice. Fourteen days after inoculation, representative macroscopic tumor images were taken (left), and the tumor weight was measured (right; $n = 6$). *B*) B16F10 WT tumor-bearing mice were treated with the Plm inhibitor YO2 or left untreated starting from d 4. On d 12, representative tumor images were taken (left) and the tumor weight determined ($n = 6$). *C*) Macroscopic image of tumor-bearing mice (left) and tumor weight of mice injected with siLRP1

(*continued on next page*)

to a 2-fold increase in tumor weight (Fig. 5*H, I*). Co-OE of LRP1 and tPA resulted in a 4-fold increase in tumor weight in injected mice. In contrast, single OE of tPA and LRP1 KD or LRP1 OE and tPA KD did not increase primary tumor growth (Fig. 5*J*). These data indicate that LRP1 and tPA restoration in low-expressing B16F1 cells generates cells with a higher proliferative capacity.

Tumor samples were retrieved on d 12, and gene expression was determined by qPCR (Fig. 5*K*). High *LRP1* and M*MP9* expression was found in tPA OE when compared with mock tumors, as determined by qPCR and Western blot analysis (Fig. 5*L*). Similarly, increased *tPA* and *MMP9* expression was detectable in LRP1 OE tumors when compared to mock controls. The highest *tPA* and *MMP9* gene and protein expression was found in tPA/LRP1 co-OE tumors (Fig. 5*K, L*). Consistent with these data, increased tPA and MMP9 plasma levels were found in mice injected with tPA/LRP1 OE tumor cells, as determined by ELISA (Fig. 5*M*). Because tPA can render Plg into its active form, Plm, we tested PAP complex levels in circulation, as an indicator of plasmin activation. The highest PAP levels were found in mice injected with B16F1 cells coexpressing tPA and LRP1 (Fig. 5*M*), suggesting that the introduction of LRP1 and tPA had changed protease secretion from cancer cells.

Proteases are involved in tumor metastasis. Thus, given the increases in proteolytic activity after cointroduction of LRP1 and tPA in B16F1 cells, we next used a lung metastasis model to determine the role of LRP1 and tPA in the metastatic process. When compared to mock cell-injected mice, mice injected with tPA or LRP1 OE tumor cells developed more lung nodules, as a measure of lung metastasis (Fig. 5*N*). Mice injected with tumor cells coexpressing both LRP1 and tPA showed massive lung metastasis. No, or very few lung metastasis, were found after intravenous injection of LRP1 OE, but tPA KD B16F1 cells or tPA OE, but LRP1 KD B16F1 cells. These data suggest that LRP1 in cooperation with tPA on tumor cells enhances lung metastasis.

Tumor-derived tPA increases tumor-residing MSCs

tPA protein expression was higher in B16F10 than in B16F1 cells, as determined by Western blot analysis (**Fig. 6*A***), corroborating the mRNA expression level (Fig. 1*A*). $Sca1^+$ MSCs form a main component of the melanoma stroma (25). Because tPA administration expands $Sca1^+$ MSCs in noncancerous organ tissues (27, 36), we wondered whether tumor MSC homeostasis is regulated by tPA. MSCs were identified by using the marker profile $CD45^-$ $Ter119^-Sca1^+PDGFR\alpha^+$ and were obtained *via* FACS. To investigate whether tPA plays a role in MSC migration, a key metastatic phenotype, MSCs were cultured in the presence of conditioned medium derived from B16F10 or B16F1 cells. In a scratch assay, bone marrow–derived MSCs migrated faster in conditioned medium derived from B16F10 than in that from B16F1 cells (Fig. 6*B*). siLRP1 silencing in WT and tPA-treated B16F10 cells prevented cell migration (Fig. 6*B*). Higher MSC counts were found in high tPA-expressing B16F10 cells, but not in low tPA-expressing B16F1-derived tumors (Fig. 6*C*). These data show that factors released from B16F10, but not B16F, cells enhance MSC recruitment.

Genetic inactivation of tumor but not niche cell tPA blocks MSC recruitment

To evaluate the contribution of niche-derived tPA in regulating the number of tumor MSCs, we injected B16F10 and B16F1 cells subcutaneously into tPA KO mice. No difference in the number of tumor-residing MSCs (Fig. 6*C*) was observed in B16F10 and B16F1 injected tPA KO when compared to the number in WT mice, indicating that tumor-, rather than niche cell–derived, factors contribute to MSC accumulation in the tumor.

To investigate whether tumor-derived tPA regulates MSC recruitment *in vivo*, tPA OE, tPA KD, and mock cells were injected into WT mice. The frequency of MSC was increased in tPA OE and reduced in tPA KD tumors when compared to mock control tumors (Fig. 6*D*). These data suggest that tumor-derived tPA controls the number of tumor-residing MSCs.

Because LRP1 can form complexes with $PDGFR^+$ cells, and MSC express PDGFRα critical for tPA-driven MSC expansion (27), we tested the *in vivo* effect of LRP1 silencing and Plm inhibition by using YO2 for MSC recruitment. The frequency of MSC was significantly reduced in siLRP1 tumors compared to si-Ctrl tumors and in tumors derived from the Plm inhibitor YO2-treated mice (Fig. 6*E*). These data suggest that tumor-derived tPA and LRP1 presence on tumor cells are essential for MSC recruitment, a process that requires active Plm.

LRP1 inhibition enhances BTZ sensitivity in B16F10 melanoma cell growth

To investigate the possibility that tumor cells modulate tPA and LRP1 expression to evade drug-induced cell death and that tPA-LRP1 signaling may contribute to BTZ resistance in melanoma cells, we treated melanoma cells with the ubiquitin-proteasome inhibitor BTZ, shown to be beneficial in animal studies for the treatment of melanoma (37). BTZ treatment prevented cell proliferation in a

and siCtrl B16F10 cells ($n = 6$). *D*) Representative hematoxylin and eosin stained tumor tissues of d 12 tumors. Scale bars, 20 (lower panels) and 200 μm (upper panels). *E*) tPA, MMP9, and PAP complex levels were quantified by ELISA in plasma of d 12 tumor-bearing mice ($n = 6$/group). *F*) Representative zymogram demonstrating MMP9 activity in plasma samples taken from tumor-bearing mice by d 12. *G, H*) Quantification of tumor nodules (left) and representative images (right) showing grossly dissected mouse lungs with lung metastasis occurring in mice after tail vein injection of siLRP1/siCtrl tPA OE (*G*), tPA KD, and mock B16F10 cells (*H*) ($n = 6$/group), or siLRP1/siCtrl B16F1 cells ($n = 3$/group). Graphs show means ± SEM. $^*P \leq 0.05$, $^{**}P \leq 0.01$ (Student's *t* test).

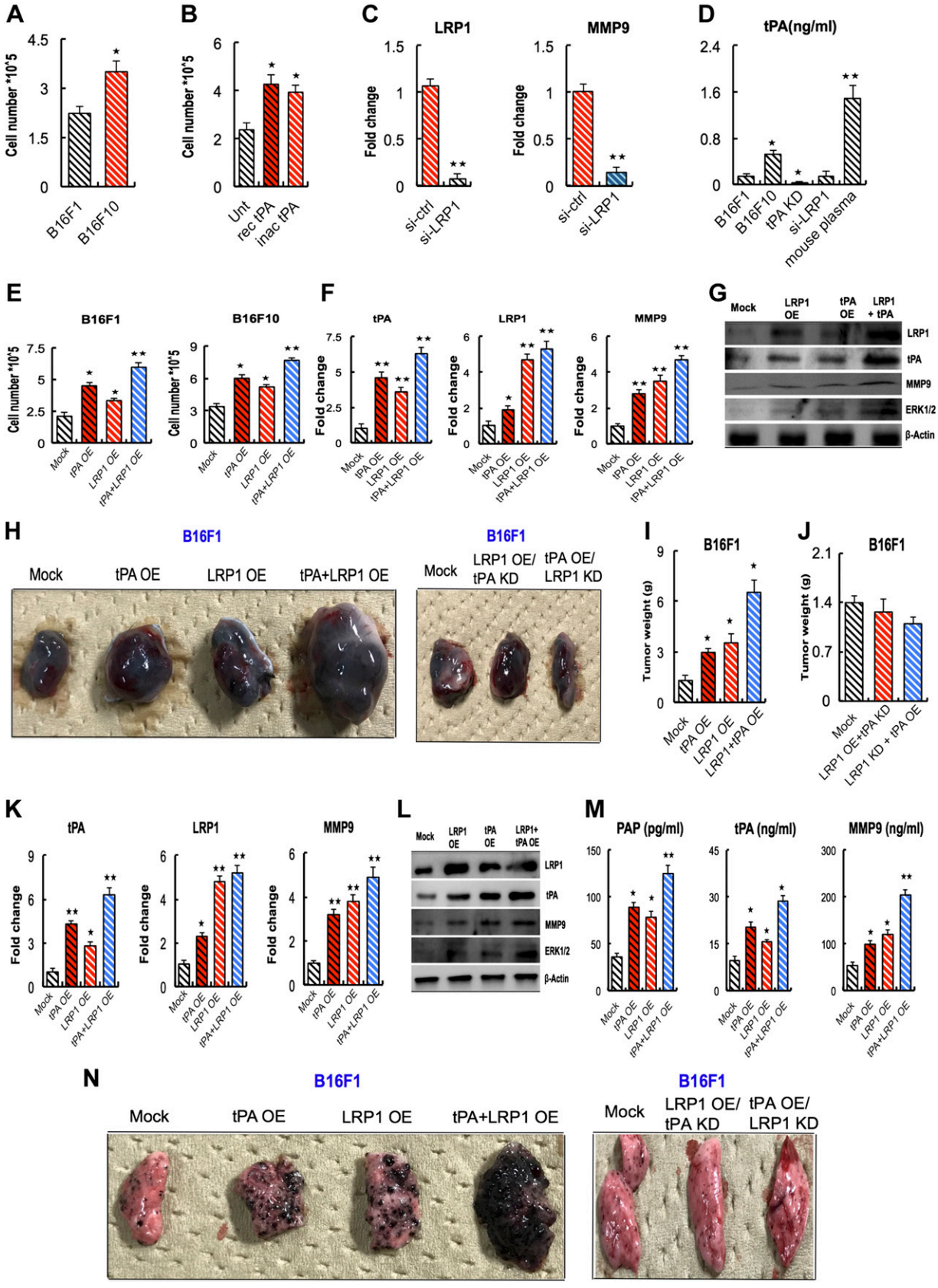

Figure 5. LRP1 and tPA overexpression enhance melanoma proliferation and lung metastasis. *A*) B16F1 and B16F10 cells were cultured for 24 h. Viable cells were counted by using trypan blue staining ($n = 6$/group). *B*) B16F1 cells were cultured with or without recombinant active or inactive tPA. Cells were counted after 24 h. Viable cells were counted using trypan blue stain ($n = 6$/group). *C*) siRNA silencing of LRP1 in B16F1 cells led to down-regulation of *LRP1* and *MMP9* expression as determined by

(*continued on next page*)

dose-dependent manner (**Fig. 7*A***) and augmented tPA and LRP1 expression, on both the mRNA and protein levels, as shown using immunofluorescent cellular staining (Fig. 7*B, C*) on treated B16F10 cells. BTZ sensitivity was significantly improved in LRP1 gene-silenced cells (Fig. 7*D*), suggesting that BTZ induced LRP1 up-regulation contributes to BTZ resistance and tPA-OE cells were more resistant to BTZ than mock cells.

Our data indicate that tPA exerted protumor functions with enhanced growth and lung metastasis *via* LRP1 that leads to the downstream activation of ERK1/2. Our molecular and *in vivo* studies revealed a role for endogenous cancer-derived tPA in the modulation of MSC recruitment through the activation of the tPA-LRP1 axis (Fig. 7*E*).

DISCUSSION

To date, most studies have focused on the fibrinolysis-promoting role of tPA in cancer. However, one study has clearly demonstrated that tPA modulates the cell behavior and cellular composition of the tumor (26). High tPA expression levels have been reported in human melanoma. In melanoma, the role and impact of tPA expression remained unclear. We found that tPA enhanced melanoma cell proliferation and migration through the membrane protein LRP1 receptor. Our identification of the tPA-LRP1 pathway highlights the significance of this ligand-receptor pair as a key modulator of melanoma tumorigenesis and metastatic progression. tPA acting on melanoma cell LRP1 receptor augments melanoma proliferation and melanoma invasion. Blockade of LRP1 on melanoma cells prevented MSC recruitment. Our results from loss- and gain-of-function analyses give rise to a model wherein tPA-LRP1 interactions through ERK1/2 to regulate the proteolytic niche within the tumor, including tPA and MMP9; changes the MSC content; and possibly changes immunoresponsiveness (should be evaluated in future studies) and controls tumor cell growth and metastasis (Fig. 7*E*).

Despite recent clinical data on overall survival benefit in patients with metastatic melanoma receiving vemurafenib or ipilimumab (38), there are still no treatments aimed at preventing metastasis. In accordance with a previous study (35), we showed that tumor-derived tPA through LRP1 controls lung metastasis, indicating that both factors are significant predictors of melanoma cancer progression. We showed that reintroduction of tPA and LRP1 generated tumor cells with high metastatic potential and with increased proliferative capacity. Tumor cells up-regulated both factors after chemotherapy, and silencing LRP1 on melanoma cells improved drug sensitivity, suggesting that LRP1 contributes to drug resistance. These data open new therapeutic windows to overcoming drug resistance.

Both overexpression and knockdown of tPA or LRP1 affected cell proliferation. Although we have observed enhanced tumor cell migration and metastasis in tPA or LRP1 OE cells, it is possible that the effects on migration and metastasis are influenced by the effect of the tPA-LRP1 axis on cell proliferation.

In our molecular experiments, tPA enhanced the release of enzymatic activity of MMP9 from tumor cells and that tPA, through MMP9, promoted melanoma cell proliferation. Increased MMP9 and -2 expression has been strongly associated with melanoma metastasis and invasion (39–41). LRP1 up-regulation led to ERK1/2 activation and improved proliferation. The mitogenic effect of tPA described for melanoma cells in our study has been reported in fibroblasts and is similar to data shown in our study that depend on the phosphorylation of Tyr4507 within the distal NPXY motif of LRP1. This effect has been demonstrated to initiate a cascade of proliferative signaling events involving phosphorylation of Erk1/2, p90RSK, and GSK3β and induction of cyclin D1 (16, 32, 42). Our data are in accordance with a recent report demonstrating that yes-associated protein, independent of hippo activation, controls melanoma growth by altering LRP1 expression with LRP1 knockdown impairing melanoma proliferation (24, 43).

Our identification of LRP1 as a regulator of melanoma cell proliferation and MSC accumulation and its dependence on the fibrinolytic pathway highlights the significance of this gene (44), but how can the tPA-LRP1 pathway promote MSC accumulation? tPA-Plm–induced cleavage and shedding of LRP1 can initiate LRP1-dependent signaling (45, 46). By increasing systemic tPA levels *in vivo*, we previously reported that tPA expands MSC in benign tissues, like the bone marrow through PDGFRα activation (27). PDGFRα was one of the surface markers used in the current study to identify tumor-infiltrating MSCs. Given

qPCR (n = 3/group/experiment; the experiment was repeated twice). *D*) tPA was measured in supernatants of sitPA KD or siLRP1 KD B16F10 cells, B16F1 WT (WT) or B16F10 WT cells, and cell-free cultures supplemented with mouse plasma by ELISA (n = 5/group). *E*) Cell proliferation was determined *in vitro* after 24 h in B16F1 (left) and B16F10 (right) of mock controls and tPA OE, LRP1 (LRP1 OE), both tPA and LRP1 (tPA OE and LRP1 OE) cells (n = 6/group). *F*) *tPA*, *LRP1*, and *MMP9* expression was determined in tumor samples of mock, tPA OE, LRP1 OE, and tPA LRP1 OE B16F1 cell-injected mice by qPCR (n = 3/group). Transcript levels were normalized to β-actin. The data represent 2 independent experiments with similar results. *G*) Western blot analysis of indicated proteins was performed on B16F1 cell lines. Two independent experiments; representative blot is shown. *H–M*) tPA OE, tPA+LRP1 OE, LRP1 OE or mock B16F1 cells were injected subcutaneously into C57Bl6/J mice (n = 3/group). Tumor samples were collected at d 12 after injection. *H*) Representative macroscopic images of B16F1 tumors retrieved by d 12 in indicated groups. *I, J*) Tumor weight of mice injected subcutaneously with different sets of transfected B16F1 cells is given (n = 3/group). *K*) tPA, LRP1, and MMP9 expression was determined in tumor samples of indicated groups using qPCR (n = 6/group). *L*) Tumor lysates extracted by d 12 were subjected to Western blotting. Representative blots showing LRP1, tPA, MMP9, ERK1/2 and b-Actin are given. *M*) Plasma tPA, MMP9, and PAP (as a measure of active plasmin) were determined by ELISA at d 12 (n = 3/group). *N*) Mice were injected intravenously with tPA OE, LRP1 OE or tPA LRP1 OE B16F1 cells (n = 3/group). Representative images were taken of lungs demonstrating lung metastasis. Data are means ± SEM. $*P \leq 0.05$, $**P \leq 0.01$.

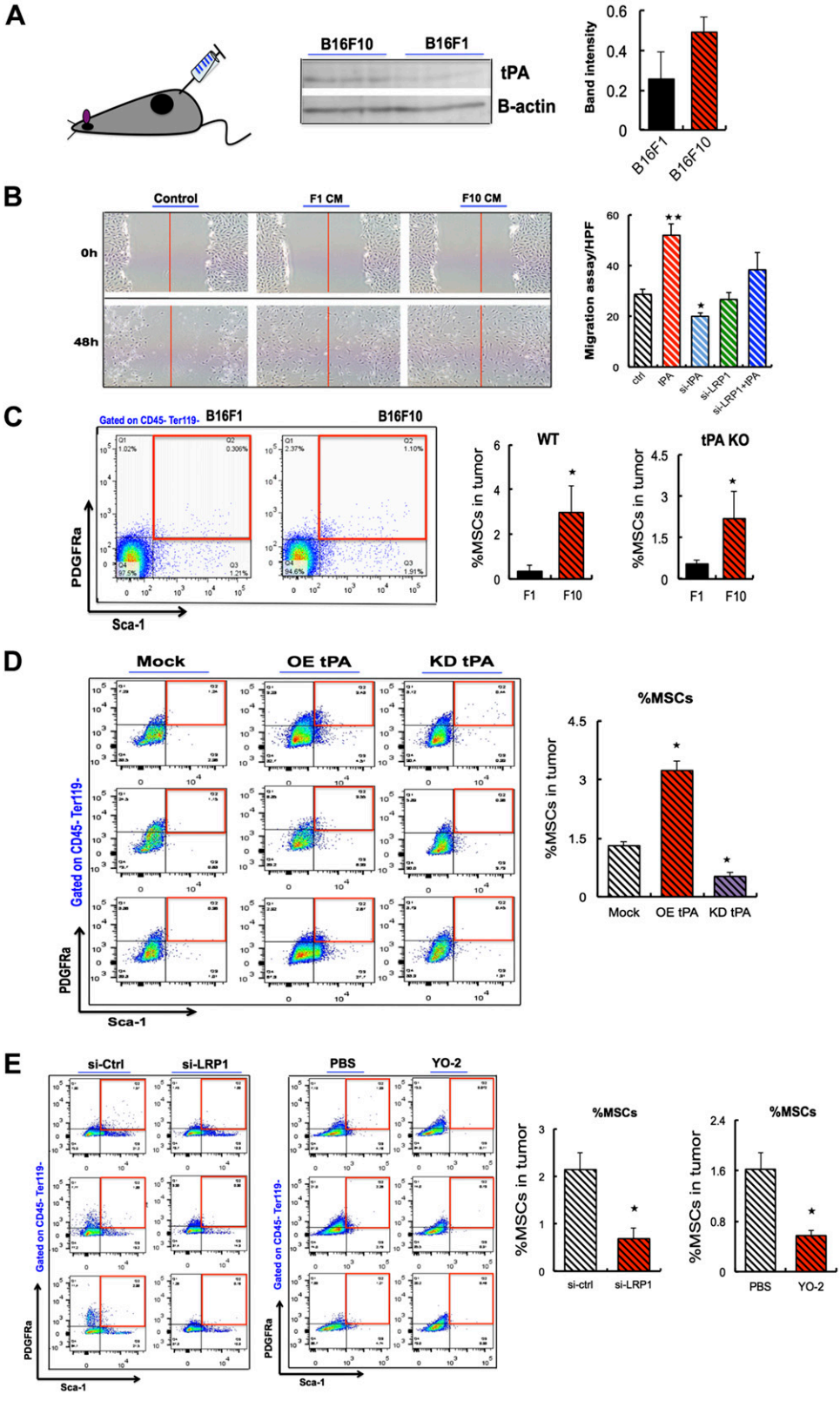

Figure 6. Melanoma-derived tPA enhances MSC recruitment. *A*) tPA levels were assessed in B16F10 and B16F1 cell lysates by Western blot analysis, and band density was quantified. *B*) Faster wound closure in MSC cultures supplemented with conditioned medium of B16F10, but not B16F1 cells as determined using a scratch assay. Images were taken 48 h after wound induction. *C*) B16F10 and B16F1 cells were injected in WT and tPA KO mice. Tumors were extracted by d 12, and the frequency of MSCs within the tumors was determined by flow cytometry with the following marker profile: $CD45^{-}Ter119^{-}PDGFRa^{+}Sca1^{+}$. *D*, *E*) MSCs in tumors were determined by FACS isolated from mice injected subcutaneously with mock, tPA OE, or tPA KD (*D*) or siLRP1/siCtrl or WT B16F10 cells (*E*). Left: representative FACS plots of tumor MSCs of the tested condition. Right: MSC frequency in the tumor. Data are means ± SEM. $^{*}P \leq 0.05$.

that LRP1 binds to the PDGFR and forms a receptor-ligand complex that activates the MAPK signaling pathway (47), PDGFR may be another LRP1 coreceptor that contributes to MSC expansion and the conversion into a tumor-promoting phenotype. Imatinib therapy targeting PDGFR in cancer-associated fibroblasts inhibits growth and metastasis of human colon cancer (48, 49). Further studies are needed to understand the role of PDGFR signaling for tPA-LRP1–induced MSC accumulation in the growing tumor and how these factors contribute to the tumor metastasis–promoting abilities of MSCs.

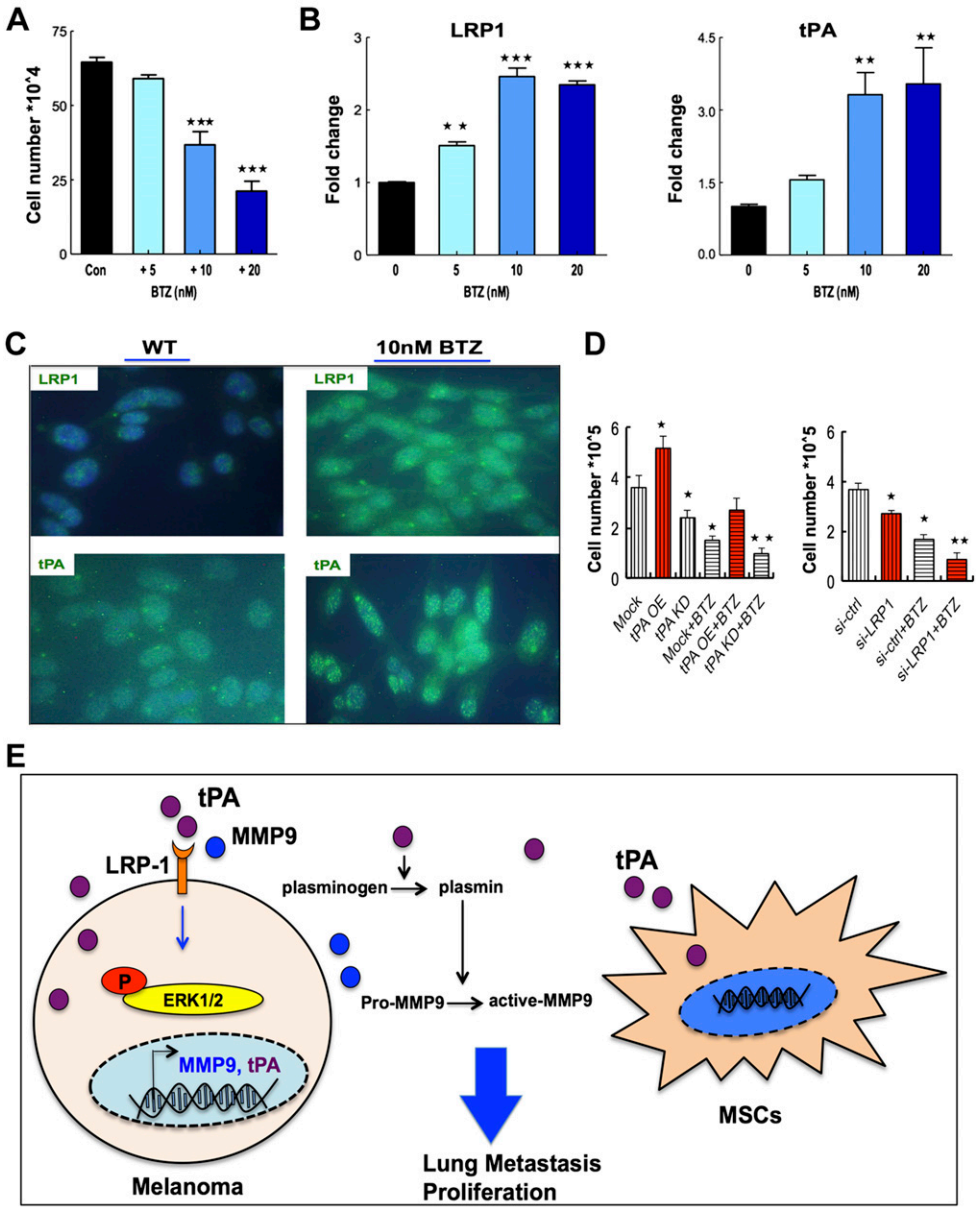

Figure 7. LRP1 loss in melanoma cells overrides BTZ resistance. *A–D*) B16F10 cells were treated at the indicated concentrations with BTZ for 24 h. A) Cell proliferation was assessed after BTZ treatment (n = 6/group). B) Relative mRNA expression of LRP1 (left) and tPA (right) after BTZ treatment in B16F10 cells (n = 6/group). *C*) LRP1 (top) and tPA (bottom) immunofluorescence was determined in cultured B16F10 cells treated with 10 nM BTZ or carrier. Representative images are shown. *D*) siLRP1 B16F10 cells and control cells were treated with 10 nM BTZ for 24 h and cell viability was determined. *E*) The effects of tPA and LRP1 on melanoma proliferation, metastasis, and MSCs within the tumor environment. Data are means ± SEM. $^*P \leq 0.05$, $^{**}P \leq 0.01$, $^{***}P \leq 0.001$.

Pencheva *et al.* (21) showed that ApoE acting on melanoma cell LRP1 receptors inhibits melanoma invasion. In contrast, our data demonstrate that tPA, which is another LRP1, ligand-enhanced migration and invasion of B16F10 melanoma cells. How can these opposing observations be reconciled, wherein two different ligands binding to the same receptor convey opposing cellular responses? The observation of 2 LRP1 ligands showing different cellular responses has been addressed in other cells—namely, neurons. Although LRP1 ligands, such as tPA, α2M, and ApoE, promote neurite outgrowth, myelin-associated glycoprotein (MAG), which also binds with high affinity to LRP1, inhibits neurite outgrowth (12). It is interesting to speculate that tPA and ApoE represent opposing drivers of melanoma metastasis, but further studies are necessary to prove this notion.

We propose that cancer cells use the promiscuity of certain receptors, such as LRP1, to mediate opposing functions. The interpretation of tumor markers like LRP1 must take into consideration the knowledge of critical ligands and coreceptors on the tumor cells itself or the niche cells, to be able to predict the biologic outcome. Our study further provides data showing that ligand-specific coreceptor recruitment allows LRP1 to function as a true sensor of the cellular microenvironment and induce different cellular changes, depending on the spectrum of available ligands. FJ

ACKNOWLEDGMENTS

This work was supported by Japan Society for the Promotion of Science Kiban (C) Grant 16K09821 (to B.H.) and Grants 16K09866, 17K09941, and 26461415 (to K.H.); Health and Labour Sciences Research Grant 24008 (to K.H); the Uehara Memorial Foundation grant (to B.H.); and the Collaborative research Fund Program for Women Researchers

from the Tokyo Medical and Dental University, funded by the Initiative for Realizing Diversity in the Research Environment, from the Ministry of Education, Culture, Sports, Science, and Technology (MEXT). The authors declare no conflicts of interest.

AUTHOR CONTRIBUTIONS

Y. Salama and B. Heissig designed and performed the experiments, analyzed the data, and wrote the manuscript; S.-Y. Lin and D. Dhahri performed some experiments; and K. Hattori provided vital reagents.

REFERENCES

1. Houghton, A. N., and Polsky, D. (2002) Focus on melanoma. *Cancer Cell* **2**, 275–278
2. Blackburn, C., Gigstad, K. M., Hales, P., Garcia, K., Jones, M., Bruzzese, F. J., Barrett, C., Liu, J. X., Soucy, T. A., Sappal, D. S., Bump, N., Olhava, E. J., Fleming, P., Dick, L. R., Tsu, C., Sintchak, M. D., and Blank, J. L. (2010) Characterization of a new series of non-covalent proteasome inhibitors with exquisite potency and selectivity for the 20S β5-subunit. *Biochem. J.* **430**, 461–476
3. De Vries, T. J., Quax, P. H., Denijn, M., Verrijp, K. N., Verheijen, J. H., Verspaget, H. W., Weidle, U. H., Ruiter, D. J., and van Muijen, G. N. (1994) Plasminogen activators, their inhibitors, and urokinase receptor emerge in late stages of melanocytic tumor progression. *Am. J. Pathol.* **144**, 70–81
4. De Vries, T. J., van Muijen, G. N., and Ruiter, D. J. (1996) The plasminogen activation system in melanoma cell lines and in melanocytic lesions. *Melanoma Res.* **6**, 79–88
5. Hofmann, U. B., Westphal, J. R., Van Muijen, G. N. P., and Ruiter, D. J. (2000) Matrix metalloproteinases in human melanoma. *J. Invest. Dermatol.* **115**, 337–344
6. Hoal-Van Helden, E. G., Wilson, E. L., and Dowdle, E. B. (1986) Characterization of seven human melanoma cell lines: melanogenesis and secretion of plasminogen activators. *Br. J. Cancer* **54**, 287–295
7. Larsen, G. R., Henson, K., and Blue, Y. (1988) Variants of human tissue-type plasminogen activator. Fibrin binding, fibrinolytic, and fibrinogenolytic characterization of genetic variants lacking the fibronectin finger-like and/or the epidermal growth factor domains. *J. Biol. Chem.* **263**, 1023–1029
8. Ortiz-Zapater, E., Peiró, S., Roda, O., Corominas, J. M., Aguilar, S., Ampurdanés, C., Real, F. X., and Navarro, P. (2007) Tissue plasminogen activator induces pancreatic cancer cell proliferation by a non-catalytic mechanism that requires extracellular signal-regulated kinase 1/2 activation through epidermal growth factor receptor and annexin A2. *Am. J. Pathol.* **170**, 1573–1584
9. Lillis, A. P., Van Duyn, L. B., Murphy-Ullrich, J. E., and Strickland, D. K. (2008) LDL receptor-related protein 1: unique tissue-specific functions revealed by selective gene knockout studies. *Physiol. Rev.* **88**, 887–918
10. Herz, J., and Strickland, D. K. (2001) LRP: a multifunctional scavenger and signaling receptor. *J. Clin. Invest.* **108**, 779–784
11. Egeblad, M., and Werb, Z. (2002) New functions for the matrix metalloproteinases in cancer progression. *Nat. Rev. Cancer* **2**, 161–174
12. Mantuano, E., Lam, M. S., and Gonias, S. L. (2013) LRP1 assembles unique co-receptor systems to initiate cell signaling in response to tissue-type plasminogen activator and myelin-associated glycoprotein. *J. Biol. Chem.* **288**, 34009–34018
13. Hahn-Dantona, E., Ruiz, J. F., Bornstein, P., and Strickland, D. K. (2001) The low density lipoprotein receptor-related protein modulates levels of matrix metalloproteinase 9 (MMP-9) by mediating its cellular catabolism. *J. Biol. Chem.* **276**, 15498–15503
14. Sánchez, M. C., Chiabrando, G. A., and Vides, M. A. (2001) Pregnancy zone protein-tissue-type plasminogen activator complexes bind to low-density lipoprotein receptor-related protein (LRP). *Arch. Biochem. Biophys.* **389**, 218–222
15. Bizik, J., Trancikova, D., Felnerova, D., Verheijen, J. H., and Vaheri, A. (1997) Spatial orientation of tissue-type plasminogen activator bound at the melanoma cell surface. *Biochem. Biophys. Res. Commun.* **239**, 322–328
16. Song, H., Li, Y., Lee, J., Schwartz, A. L., and Bu, G. (2009) Low-density lipoprotein receptor-related protein 1 promotes cancer cell migration and invasion by inducing the expression of matrix metalloproteinases 2 and 9. *Cancer Res.* **69**, 879–886
17. Lin, L., and Hu, K. (2014) LRP-1: functions, signaling and implications in kidney and other diseases. *Int. J. Mol. Sci.* 15, 22887–22901
18. Wang, X., Lee, S. R., Arai, K., Tsuji, K., Rebeck, G. W., and Lo, E. H. (2003) Lipoprotein receptor-mediated induction of matrix metalloproteinase by tissue plasminogen activator. *Nat. Med.* **9**, 1313–1317886
19. Hu, K., Wu, C., Mars, W. M., and Liu, Y. (2007) Tissue-type plasminogen activator promotes murine myofibroblast activation through LDL receptor-related protein 1-mediated integrin signaling. *J. Clin. Invest.* **117**, 3821–3832
20. Xing, P., Liao, Z., Ren, Z., Zhao, J., Song, F., Wang, G., Chen, K., and Yang, J. (2016) Roles of low-density lipoprotein receptor-related protein 1 in tumors. *Chin. J. Cancer* **35**, 6
21. Pencheva, N., Tran, H., Buss, C., Huh, D., Drobnjak, M., Busam, K., and Tavazoie, S. F. (2012) Convergent multi-miRNA targeting of ApoE drives LRP1/LRP8-dependent melanoma metastasis and angiogenesis. *Cell* **151**, 1068–1082
22. De Vries, T. J., Verheijen, J. H., de Bart, A. C., Weidle, U. H., Ruiter, D. J., and van Muijen, G. N. (1996) Decreased expression of both the low-density lipoprotein receptor-related protein/alpha(2)-macroglobulin receptor and its receptor-associated protein in late stages of cutaneous melanocytic tumor progression. *Cancer Res.* **56**, 1432–1439
23. Yamamoto, M., Ikeda, K., Ohshima, K., Tsugu, H., Kimura, H., and Tomonaga, M. (1997) Increased expression of low density lipoprotein receptor-related protein/alpha2-macroglobulin receptor in human malignant astrocytomas. *Cancer Res.* **57**, 2799–2805
24. Xiong, H., Yu, Q., Gong, Y., Chen, W., Tong, Y., Wang, Y., Xu, H., and Shi, Y. (2017) Yes-associated protein (YAP) promotes tumorigenesis in melanoma cells through stimulation of low-density lipoprotein receptor-related protein 1 (LRP1). *Sci. Rep.* **7**, 15528
25. Treviño-Villarreal, J. H., Cotanche, D. A., Sepúlveda, R., Bortoni, M. E., Manneberg, O., Udagawa, T., and Rogers, R. A. (2011) Host-derived pericytes and Sca-1+ cells predominate in the MART-1-stroma fraction of experimentally induced melanoma. *J. Histochem. Cytochem.* **59**, 1060–1075
26. Heissig, B., Eiamboonsert, S., Salama, Y., Shimazu, H., Dhahri, D., Munakata, S., Tashiro, Y., and Hattori, K. (2016) Cancer therapy targeting the fibrinolytic system. *Adv. Drug Deliv. Rev.* **99**, 172–179
27. Dhahri, D., Sato-Kusubata, K., Ohki-Koizumi, M., Nishida, C., Tashiro, Y., Munakata, S., Shimazu, H., Salama, Y., Eiamboonsert, S., Nakauchi, H., Hattori, K., and Heissig, B. (2016) Fibrinolytic crosstalk with endothelial cells expands murine mesenchymal stromal cells. *Blood* **128**, 1063–1075
28. Kanegae, Y., Makimura, M., and Saito, I. (1994) A simple and efficient method for purification of infectious recombinant adenovirus. *Jpn. J. Med. Sci. Biol.* **47**, 157–166
29. Enomoto, R., Sugahara, C., Komai, T., Suzuki, C., Kinoshita, N., Hosoda, A., Yoshikawa, A., Tsuda, Y., Okada, Y., and Lee, E. (2004) The structure-activity relationship of various YO compounds, novel plasmin inhibitors, in the apoptosis induction. *Biochim. Biophys. Acta* **1674**, 291–298
30. Tsuda, Y., Tada, M., Wanaka, K., Okamoto, U., Hijikata-Okunomiya, A., Okamoto, S., and Okad, Y. (2001) Structure-inhibitory activity relationship of plasmin and plasma kallikrein inhibitors. *Chem. Pharm. Bull. (Tokyo)* **49**, 1457–1463
31. Cillo, C., Dick, J. E., Ling, V., and Hill, R. P. (1987) Generation of drug-resistant variants in metastatic B16 mouse melanoma cell lines. *Cancer Res.* **47**, 2604–2608
32. Lin, L., Bu, G., Mars, W. M., Reeves, W. B., Tanaka, S., and Hu, K. (2010) tPA activates LDL receptor-related protein 1-mediated mitogenic signaling involving the p90RSK and GSK3β pathway. *Am. J. Pathol.* **177**, 1687–1696
33. Zhao, Y., Li, D., Zhao, J., Song, J., and Zhao, Y. (2016) The role of the low-density lipoprotein receptor-related protein 1 (LRP-1) in regulating blood-brain barrier integrity. *Rev. Neurosci.* **27**, 623–634
34. Hu, K., Yang, J., Tanaka, S., Gonias, S. L., Mars, W. M., and Liu, Y. (2006) Tissue-type plasminogen activator acts as a cytokine that triggers intracellular signal transduction and induces matrix metalloproteinase-9 gene expression. *J. Biol. Chem.* **281**, 2120–2127
35. Alizadeh, H., Ma, D., Berman, M., Bellingham, D., Comerford, S. A., Gething, M.-J. H., Sambrook, J. F., and Niederkorn, J. Y. (1995) Tissue-type

plasminogen activator-induced invasion and metastasis of murine melanomas. *Curr. Eye Res.* **14**, 449–458
36. Heissig, B., Lund, L. R., Akiyama, H., Ohki, M., Morita, Y., Rømer, J., Nakauchi, H., Okumura, K., Ogawa, H., Werb, Z., Danø, K., and Hattori, K. (2008) The plasminogen fibrinolytic pathway is required for hematopoietic regeneration. *Cell Stem Cell* **1**, 658–670; erratum: **3**, 120
37. Poklepovic, A., Youssefian, L. E., Winning, M., Birdsell, C. A., Crosby, N. A., Ramakrishnan, V., Ernstoff, M. S., and Roberts, J. D. (2013) Phase I trial of bortezomib and dacarbazine in melanoma and soft tissue sarcoma. *Invest. New Drugs* **31**, 937–942; erratum: 1095
38. Hutchinson, L. (2015) Skin cancer: golden age of melanoma therapy. *Nat. Rev. Clin. Oncol.* **12**, 1
39. Coussens, L. M., Tinkle, C. L., Hanahan, D., and Werb, Z. (2000) MMP-9 supplied by bone marrow-derived cells contributes to skin carcinogenesis. *Cell* **103**, 481–490
40. Hofmann, U. B., Westphal, J. R., Waas, E. T., Zendman, A. J., Cornelissen, I. M., Ruiter, D. J., and van Muijen, G. N. (1999) Matrix metalloproteinases in human melanoma cell lines and xenografts: increased expression of activated matrix metalloproteinase-2 (MMP-2) correlates with melanoma progression. *Br. J. Cancer* **81**, 774–782
41. MacDougall, J. R., Bani, M. R., Lin, Y., Muschel, R. J., and Kerbel, R. S. (1999) 'Proteolytic switching': opposite patterns of regulation of gelatinase B and its inhibitor TIMP-1 during human melanoma progression and consequences of gelatinase B overexpression. *Br. J. Cancer* **80**, 504–512
42. Fayard, B., Bianchi, F., Dey, J., Moreno, E., Djaffer, S., Hynes, N. E., and Monard, D. (2009) The serine protease inhibitor protease nexin-1 controls mammary cancer metastasis through LRP-1-mediated MMP-9 expression. *Cancer Res.* **69**, 5690–5698
43. Feng, X., Degese, M. S., Iglesias-Bartolome, R., Vaque, J. P., Molinolo, A. A., Rodrigues, M., Zaidi, M. R., Ksander, B. R., Merlino, G., Sodhi, A., Chen, Q., and Gutkind, J. S. (2014) Hippo-independent activation of YAP by the GNAQ uveal melanoma oncogene through a trio-regulated rho GTPase signaling circuitry. *Cancer Cell* **25**, 831–845
44. Strickland, D. K., Gonias, S. L., and Argraves, W. S. (2002) Diverse roles for the LDL receptor family. *Trends Endocrinol. Metab.* **13**, 66–74
45. Polavarapu, R., Gongora, M. C., Yi, H., Ranganthan, S., Lawrence, D. A., Strickland, D., and Yepes, M. (2007) Tissue-type plasminogen activator-mediated shedding of astrocytic low-density lipoprotein receptor-related protein increases the permeability of the neurovascular unit. *Blood* **109**, 3270–3278
46. Maeda, S., Nakajima, K., Tohyama, Y., and Kohsaka, S. (2009) Characteristic response of astrocytes to plasminogen/plasmin to upregulate transforming growth factor beta 3 (TGFbeta3) production/secretion through proteinase-activated receptor-1 (PAR-1) and the downstream phosphatidylinositol 3-kinase (PI3K)-Akt/PKB signaling cascade. *Brain Res.* **1305**, 1–13
47. Muratoglu, S. C., Mikhailenko, I., Newton, C., Migliorini, M., and Strickland, D. K. (2010) Low density lipoprotein receptor-related protein 1 (LRP1) forms a signaling complex with platelet-derived growth factor receptor-beta in endosomes and regulates activation of the MAPK pathway. *J. Biol. Chem.* **285**, 14308–14317
48. Shinagawa, K., Kitadai, Y., Tanaka, M., Sumida, T., Onoyama, M., Ohnishi, M., Ohara, E., Higashi, Y., Tanaka, S., Yasui, W., and Chayama, K. (2013) Stroma-directed imatinib therapy impairs the tumor-promoting effect of bone marrow-derived mesenchymal stem cells in an orthotopic transplantation model of colon cancer. *Int. J. Cancer* **132**, 813–823
49. Nwani, N. G., Deguiz, M. L., Jimenez, B., Vinokour, E., Dubrovskyi, O., Ugolkov, A., Mazar, A. P., and Volpert, O. V. (2016) Melanoma cells block PEDF production in fibroblasts to induce the tumor-promoting phenotype of cancer-associated fibroblasts. *Cancer Res.* **76**, 2265–2276

Received for publication June 30, 2018.
Accepted for publication October 15, 2018.